

MODELING OF OPTO-ACOUSTIC GAS ANALYZER WITH A HEAT SOURCE FOR MEASURING MULTICOMPONENT GAS MIXTURES

V. A. Kapitanov, M.Yu. Kataev, A.A. Mitsel', B.A. Tikhomirov, and K.M. Firsov

*Institute of Atmospheric Optics,
Siberian Branch of the Russian Academy of Sciences, Tomsk
Received December 28, 1991*

The potentialities of the OA gas analyzer with thermal excitation for measuring the concentrations of CO, NO₂, and NO in a dried mixture of N₂ + CO₂ + CH₄ + H₂O are numerically modeled. The problems of optimizing the parameters of the illuminating system and modeling the absorption coefficients of gases in the OAC cell and minimum detectable gas concentrations are considered, and the result of solving the inverse problem are presented. The possibilities of detecting the NO₂ at a level of ~ 2 mg/m³ with a radiation power of 1 mW and NO and CO at the levels of 2 mg/m³ with a radiation power of 10 mW are shown.

1. INTRODUCTION

The opto-acoustic (OA) gas analyzer has a number of advantages over the other optical devices for measuring gas mixture composition, first of all, high absorption sensitivity ($10^{-7} - 10^{-9} \text{ cm}^{-1}$), small overall dimensions, and low energy consumption.

The present paper is concerned with modeling the capabilities of the thermally excited OA gas analyzer for measuring the concentration of such gases as CO, NO₂, and NO in the dried mixture of N₂ (0.888), CO₂ (0.1), CH₄ (0.01), and H₂O ($0.156 \cdot 10^{-3} \text{ atm}$). The following problems are discussed: formation of a radiation flux incident on a light filter from a spherical source being placed at the focus of an ellipsoidal reflector, study of the transmission band shape of the interference light filter in this illumination scheme, and modeling the absorption coefficients of gases in the OAC cell and limiting detectable gas concentration as well as the solution of the inverse problem.

In the optically thin layer approximation in the OA cell the relation for the OA signal has the form¹

$$U = \eta \int W(\nu) \left[\sum_{j=1}^m \kappa_j(\nu) \rho_j + \beta_f \right] d\nu, \quad (1)$$

where η is the constant of the OAC cell, $W(\nu)$ is the radiation power upon entering the OA cell, ρ_j is the j th gas concentration in the mixture, $\kappa_j(\nu)$ is the j th gas absorption coefficient at the frequency ν , β_f is the background absorption coefficient, and m is the number of absorbing gases in the mixture.

The molecular absorption coefficient can be written as

$$\kappa_j(\nu) = \sum_i S_{ij} F(\nu, \nu_{ij}), \quad (2)$$

where S_{ij} and ν_{ij} are the intensity and the position of the centre of the i th spectral line of the j th gas and $F(\nu, \nu_{ij})$ is the i th line shaping factor normalized to unity. In view of the fact that the absorption linewidth is much narrower than the width of the radiation spectrum for a heat source, relation (1) on account of Eq. (2) can easily be reduced to a form

$$U = \eta W_0 \left[\sum_{j=1}^m K_j \rho_j + \beta_f \right], \quad (3)$$

where $K_j = \sum_i g(\nu_{ij}) S_{ij}$, $g(\nu)$ is the OA gas analyzer instrumental function normalized to unity which is related to $W(\nu)$ via the formula $g(\nu) = W(\nu)/W_0$ and W_0 is the integral intensity upon entering the OA cell.

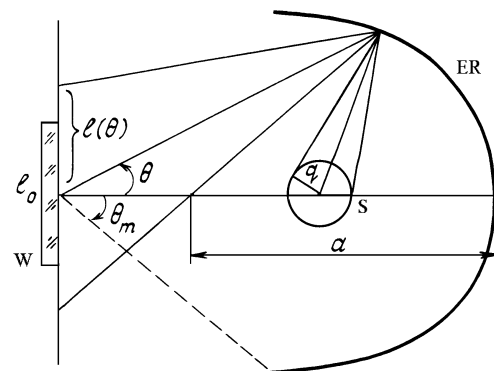


FIG. 1. Scheme of the illuminating system: S is the source of the IR radiation, ER is the elliptical reflector, W is the window of the OA cell, l_0 is the radius of the OA cell, q is the radius of the spherical source of the IR radiation, a is the major semi-axis, and $l(\theta)$ is the radius of a light spot.

2. INSTRUMENTAL FUNCTION OF THE OA GAS ANALYZER

A signal from the OA cell is proportional to the radiation power incident on it. The usage of heat source requires such an illuminating system which makes it possible to increase the radiation power incident on the OA cell. For this to happen we may use an elliptical reflector² at the focus of which a heat source is placed while at the other focus – a receiving window of the OA cell equipped with an interference light filter for selection of a sufficiently narrow spectral interval (see Fig. 1). However, the spectral characteristics of multilayer interference systems depend on the angle of radiation incident on the

coating.³ As the angle of incident radiation increases, the maximum of transmission shifts toward the short-wave region, the characteristic decays slower, and the background grows.

At larger angles of incidence a doublet structure can be manifested due to change in optical properties of coating for *S*- and *P*-components of the incident radiation. Therefore, to calculate the spectral shape of the transmission band of the interference light filter for the foregoing scheme of illumination, one should take into account the dependence of the filter characteristics and the radiation power on the angle of light incidence

$$W(\nu) = \int \frac{dW^0}{d\theta} \tau(\nu, \theta) d\theta, \tag{4}$$

where $dW^0/d\theta$ is the angular distribution of radiation power incident on the filter surface and $\tau(\nu, \theta)$ is the light filter transmission at the frequency ν for the radiation incident at the angle θ .

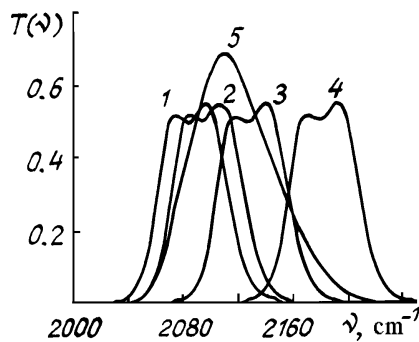


FIG. 2. Transmission band shapes of the interference light filter for different schemes of illumination.

Now it is possible to calculate the transmission band shape for a narrow-band system. However, one should have a good knowledge of the structure and materials for manufacturing the filter, which is unavailable as a rule. The nominal data of the filter usually include the following parameters: the frequency of the center of the transmission band ν_0 , the half-width at half maximum $\delta\nu_0$, and the transmission τ_0 at the center of the band at the frequency ν_0 . Moreover, the shift of maximum at the fixed angle θ_0 is sometimes included. Therefore, to describe the transmission band shape the approximate formulas were employed.

A sufficiently good approximation for the asymmetric transmission band of a narrow-band filter is the Lorentz line shape while for a symmetric band it is a Gaussian profile.² In calculations we also used a real shape of the transmission spectrum $T(\nu)$ of the filter manufactured at the Scientific-Production Union "Analitpribor". Transmission band of the light filter in the case of a perpendicular incidence of light (curve 1 in Fig. 2) was given in the nominal data.

The displacement of the transmission band maximum toward the short-wave region can be approximated by the relation³

$$\nu_0(\theta) = \sqrt{1 - \sin^2\theta/n^2}, \tag{5}$$

where n is the refractive index of a separating layer when a real bandpass system is replaced by a filter incorporating two mirrors and the separating layer between them. If we know the maximum shifts at the fixed angle, then we can

easy calculate the refractive index. The values of τ_0 and $\delta\nu_0$ were assumed to be independent of the angle θ .

To describe the angular distribution of the radiation power incident from the illuminating system on the filter surface (see Fig. 1) a sufficiently simple approximation is needed since a great number of spectral lines, which can attain several tens of thousands, is required for the absorption coefficients to be calculated. It is rather difficult to calculate light fluxes incident from one surface on the other,³ while for a point source it is easy to obtain the angular distribution of radiation power in the focal plane with a light filter placed in it

$$\frac{dW}{d\theta} = 2\pi\alpha_\nu B_\nu \frac{(1 - \epsilon^2)^2 \sin\theta}{(1 + \epsilon^2 - 2\epsilon \cos\theta)^2}, \tag{6}$$

where ϵ is the reflector eccentricity, α_ν is the spectral absorption coefficient of the material from which the radiation source is made, and B_ν is the emissivity of the point source. For a spherical source B_ν equals $S_q L_\nu$, where S_q is the source cross section and L_ν is the Planck function. Relation (6) is also valid for a spherical source if its radius is much smaller than the major semi-axis of the elliptic reflector and the transverse dimensions of the filter are larger than those of the source image. Shown in Fig. 3 is the irradiance distribution in the plane of the filter for different eccentricities of the reflector which allows one to relate the dimensions of the source and the filter.

It follows from this figure that Eq. (6) must be corrected taking into account the fact that the light filter does not intercept the entire flux. The light flux incident on the light filter at the angles from θ to $\theta + d\theta$ provides practically uniform irradiance of the area of radius

$$l(\theta) = q \frac{1 - \epsilon^2}{(1 - 2\epsilon \cos\theta + \epsilon^2) \cos\theta}. \tag{7}$$

Since the irradiance is proportional to the radiation flux incident on a unit area, the radiation flux proportional to $(l_0/l(\theta))^2$ passes through the filter within these angles, where l_0 is the light filter radius and $l(\theta)$ is determined by formula (7). Therefore, to take into account the finite size of the interference filter in Eq. (4), it is possible to introduce the correction function χ as a multiplier being equal to unity for $l(\theta) < l_0$ and to $(l_0/l(\theta))^2$ for $l(\theta) > l_0$.

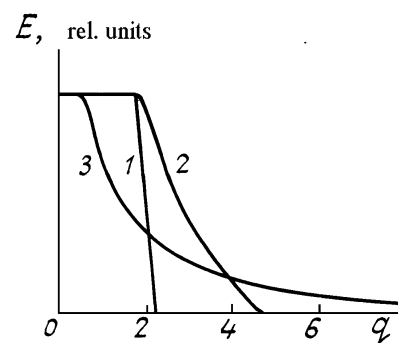


FIG. 3. Irradiance of the receiving window of the OA cell in relative units as a function of q . The reflector eccentricity: 1) $\epsilon = 0.4$, 2) $\epsilon = 0.62$; and, 3) $\epsilon = 0.85$. The maximum angle of light incident on the window is $\Theta = 33^\circ$.

Formulas (4) – (7) allows us the calculation of the instrumental function $g(\nu)$ to be made

$$g(\nu) = \frac{\int_0^{\theta_m} \frac{dW(\nu)}{d\theta} \tau(\nu, \theta) d\theta}{\int_{\Delta\nu} d\nu \int_0^{\theta_m} \frac{dW(\nu)}{d\theta} \tau(\nu, \theta) d\nu}, \quad (8)$$

which is required for the efficient absorption coefficients $K(\nu)$ in Eq. (3) to be determined. In formula (8) θ_m is the maximum angle of the light flux incident on the light filter.

Figure 2 shows the calculated transmission bands of the light filter at four angles of radiation incident on the filter: $\theta = 0, 10, 20,$ and 30° (curves 1, 2, 3, and 4, respectively) for a parallel light beam. Curve 5 shows the instrumental function normalized to unity for a focused beam incident on the light filter with the maximum incidence angle $\theta_m = 33^\circ$ produced by the elliptic reflector with the eccentricity $\varepsilon = 0.62$ at the focus of which a Lambertian spherical source of radiation is placed. The curves shown in Fig. 2 were obtained for a light filter with typical characteristics: $\nu_0 = 2100 \text{ cm}^{-1}$, $\delta\nu_0 = 32 \text{ cm}^{-1}$, a relative value of maximum displacement at $\theta = 20^\circ$ is 0.02.

To obtain a maximum signal it is necessary to optimize the choice of dimensions of the radiation source and the receiving window of the OA cell, the eccentricity, and the major semi-axis of the elliptic reflector as well as of the maximum angle of incidence θ_m shown in Fig. 1. The signal from the OA cell is proportional to the radiation power entering it which, in its turn, is proportional to the average irradiance of the window. The irradiance at the center of the light filter is proportional to $\sin^2\theta_m$ (θ_m is the maximum angle of the light incident on the filter). The maximum value of the angle θ_m must be taken $\sim 30^\circ$, since at larger angles a large displacement of the light-filter transmission band takes place, as is shown in Fig. 2, and moreover, at larger θ_m a substantial broadening of the light filter transmission band occurs, and the background level grows.³ Comprehensive analysis of conditions for light flux propagation through the light filter and OA signal formation enabled us to reveal the following tendencies: 1) the efficiency of transformation of light energy of the illumination system $\eta = \Phi_{tr}/\Phi_{inc}$ (where Φ_{tr} and Φ_{inc} are the radiation flux transmitted through the light filter and incident on it) decreases with increase of ε and decrease of the relative radius of the window l_0/q , and 2) for a fixed length of the OA cell the OA signal decreases with an increase of l_0/q and attains its extremum (maximum) in ε for a fixed value of l_0/q , and 3) with increase in ε the displacement of the transmission band maximum decreases and its width varies insignificantly. Starting from the foregoing analysis we can obtain the maximum OA signal for the following parameters of the illuminating system: $\varepsilon = 0.6 - 0.65$ and $l_0/q \approx 2.3 - 2.7$, where q is the radius of the radiation source.

3. CALCULATION OF THE ABSORPTION COEFFICIENTS

Our analysis of the absorption spectra using the database from Ref. 5 showed that the maximum absorption of gases CO, NO and NO_2 is observed within the following spectral ranges: CO – 2050–2200, NO – 1780–1930, and

NO_2 – 1530–1650 cm^{-1} . In these ranges there also exist absorption bands of other gases, such as H_2O , CO_2 , and CH_4 , which overlap with the absorption bands of the examined gases. Therefore the absorption coefficients were calculated for all of the six gases in three spectral ranges: 1500–1800, 1700–2500, and 2900–3200 cm^{-1} . A channel for sounding CO was chosen in the 2055–2200 cm^{-1} range. The basic interfering gas was carbon dioxide which has a strong absorption band centered at 4.3 μm . As is well known,² real light filters have a short-wave wing extending far away, while the model transmission band of the above-described filter was obtained disregarding this wing. In order the absorption at the center of the 4.3 μm band of CO_2 to be taken into account, a short-wave wing was modeled on the assumption of a combined light filter based on the catalogue of Ref. 7. This resulted in the fact that the optically thin gas approximation was violated at the center of the 4.3 μm band of CO_2 and the CO_2 absorption coefficient was nonlinearly dependent on its concentration. To take this effect into consideration we made use of the method described in Ref. 6. To reduce the effect of the central part of the 4.3 μm band of CO_2 , a gas filter with CO_2 inserted in the CO channel was modeled. The effect of a short-wave wing of the instrumental function was insignificant for the rest of gases. Figures 4 *a* and *b* show the absorption coefficients calculated disregarding the short-wave wing.

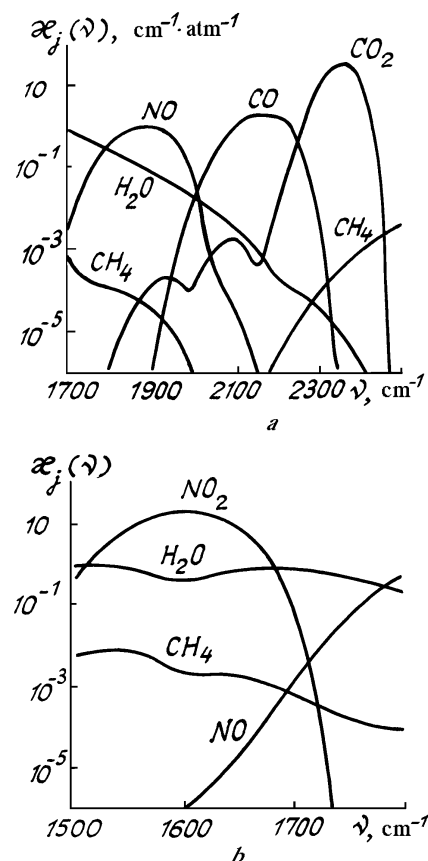


FIG. 4. The absorption coefficients without the wing of the instrumental function. The model of absorption is linear.

4. MINIMUM DETECTABLE GAS CONCENTRATIONS

To model the minimum detectable gas concentrations we employ the results of Ref. 8 where the detection algorithm was considered based on a mathematical apparatus for verifying the statistical hypothesis.⁹ Let us use the Neumann—Pearson criterion as a criterion for detection. We give here the finite formulas for calculating the minimum detectable gas concentrations.

The probability of correct detection (the detection reliability) is calculated from the formulas

$$P = \frac{1}{2} [1 + \Phi(g)], \quad (9)$$

$$g = \frac{E - \Lambda}{2\sqrt{E}}; \quad (10)$$

where

$$E = \frac{1}{2\sigma^2} (M_2 - M_1)^2; \quad (11)$$

$$\Lambda = 2\sqrt{E} \Phi^{-1}(1 - 2\varepsilon_0) - E; \quad (12)$$

$$\Phi(g) = \frac{2}{\sqrt{\pi}} \int_0^g \exp(-t^2) dt.$$

In formula (11) the parameters M_1 , M_2 , and σ have the form

$$M_1 = \eta W_0 (k_1 \rho_1 + \beta); \quad M_2 = \eta W_0 (k_2 \rho_2 + \beta); \quad (13)$$

$$\sigma^2 = \sigma_a^2 + d_{\beta}^2 (\eta W_0 \beta)^2, \quad (14)$$

where κ is the absorption coefficient of the examined gas, β is the total absorption coefficient of the interfering gases of the mixture and background, ρ_1 and ρ_2 are the concentrations of the gas in the hypotheses H_1 and H_2 , respectively. In this problem $\rho_1 = 0$, $\rho_2 = \rho$, W_0 is the radiation power of the heat source, σ_a is the absolute error in the OA signal, σ_{η} is the relative error in determining β , and ε_0 is the fixed probability of the error of the second kind.⁹ In this paper it was taken to be equal to 0.05.

The criterion for determining the minimum detectable concentration is as follows. Based on the prescribed parameters of the OA gas analyzer (η , W_0 , σ_{η} , δ_{β} , and β_{χ}), concentrations of interfering gases ρ_i , and the absorption coefficients we calculate the probability of correct detection P as a function of the wavelength and concentration of the examined gas ρ . The value of ρ for which $P \geq 0.95$ is taken to be the minimum detectable concentration ρ_{\min} . It is clear that at different wavelengths the values of P are different and, hence, the detectable concentration is different at different wavelengths.

To determine the value of ρ_{\min} the following concentrations of interfering gases were taken: CO_2 — 0.1, CH_4 — 0.01, H_2O — $0.156 \cdot 10^{-3}$, CO — $1.89 \cdot 10^{-6}$, NO_2 — $2.31 \cdot 10^{-6}$, and NO — $3.53 \cdot 10^{-6}$ atm. The parameters of the OA system were $\eta = 50 \text{ mV}/(\text{mW} \cdot \text{cm}^{-1})$, $\sigma_a = 2 \cdot 10^{-4} \text{ mV}$, $\beta_{\chi} = 5 \cdot 10^{-8} \text{ cm}^{-1}$, $W_0 = 1 - 10 \text{ mW}$, $\delta_{\beta} = 4\%$ for $W_0 = 1 \text{ mW}$ and $\delta_{\beta} = 0.4\%$ for $W_0 = 10 \text{ mW}$. The value of δ_{β} was found by solving the inverse problem (see Sec. 5), in

this case the maximum value of the relative error in determining the interfering gas concentration was taken as δ_{β} .

Shown in Fig. 5 are the absorption coefficients for the interfering and examined gases in those spectral regions which are favourable for their measurements. Figure 5a shows the values of β obtained with and without account of a short-wave transmission wing of the interference filter. Due to high CO_2 concentration in the mixture and the presence, in the given range, of a strong CO_2 band centered at 2370 cm^{-1} (Fig. 4a) the condition of an optically thin layer in the OA cell changes that results in violating the linearity of model (3). Therefore, instead of Eq. (3) a nonlinear model was employed for the coefficients β_{CO_2} to be calculated in the frequency range $2050 - 2200 \text{ cm}^{-1}$.

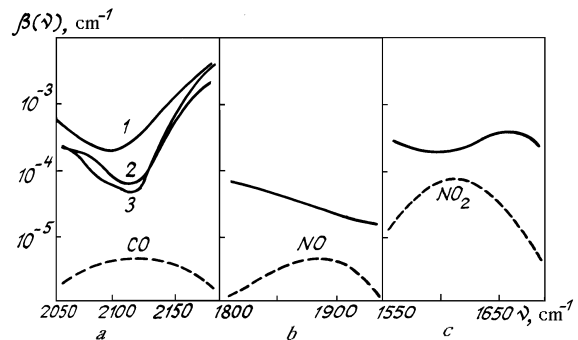


FIG. 5. The absorption coefficients of the examined (dashed curves) and interfering (solid curves) gases: a) $\rho_{\text{CO}} = 2 \text{ mg}/\text{m}^3$, with an account of the short-wave wing of the instrumental function (1); without the wing (2); with an account of the wing and the CO_2 gas filter (3); b) $\rho_{\text{NO}} = 4 \text{ mg}/\text{m}^3$; and, c) $P_{\text{NO}_2} = 4 \text{ mg}/\text{m}^3$.

As can be seen from Fig. 5, the most pronounced effect of interfering gases is peculiar to CO. Thus, for a filter with a wing, the minimum ratio $\beta_1/\alpha_{\text{CO}}$ for $\rho_{\text{CO}} = 2 \cdot 10^{-3} \text{ g}/\text{m}^3$ is ~ 60 at a frequency of 2100 cm^{-1} while for the filter without wing the minimum ratio $\beta_2/\alpha_{\text{CO}} = 9.6$ at the frequency $\nu = 2120 \text{ cm}^{-1}$. Shown here are the absorption coefficients of interfering gases β_3 when a CO_2 gas filter 1 cm in length at the pressure $P_{\text{CO}_2} = 1 \text{ atm}$ was inserted in the CO channel. In this case it becomes possible to reduce the effect of interfering gases by a factor of more than two in the frequency range $2100 - 2130 \text{ cm}^{-1}$.

TABLE I. Minimum detectable concentrations of gases (mg/m^3).

Frequency, cm^{-1}	Gas	$W_0 = 1 \text{ mW}$		$W_0 = 10 \text{ mW}$	
		without a wing	with a wing	without a wing	with a wing
2110	CO*	9.0	18	0.9	1.8
		9.0	9.5	0.9	0.95
1870	NO	16		1.6	
1600	NO_2	2.2		0.22	

*The denominator includes the values of r_{CO}^{\min} obtained when a CO_2 gas filter was inserted in the CO channel.

Table I lists the minimum detectable concentrations of the examined gases, in mg/m^3 , calculated for the two values of radiation power $W_0 = 1$ and 10 mW and detection reliability $P = 0.95$. It becomes apparent from the table that for the instrumental function of the light filter without far wings the gas filter does not provide any advantage in the CO detection. As the concentration of the interfering gas CO_2 becomes lower by an order of magnitude, the nonlinearity of the absorption model weakens, the detectability increases, and the center of the optimum channel for determining CO is displaced from a frequency of 2100 to 2140 cm^{-1} . At the same time, the effect of a high-frequency wing of the instrumental function of the light filter becomes insignificant. The frequency shift of the best detectability of CO can be explained by the fact that at a frequency of 2140 cm^{-1} the absorption coefficient α_{CO} attains its maximum (see Fig. 4 a).

When nitric oxides are measured in this mixture the water vapour has the most pronounced effect. Thus, e.g., the increase in the H_2O concentration by an order of magnitude deteriorates the gas analyzer detectability with respect to NO by a factor of 1.5 and with respect to NO_2 by a factor of 5.

Based on the information about the characteristics of the OA gas analyzer, the absorption coefficients of interfering gases, and their concentrations, the foregoing criterion allows one to determine the wavelength at which it is possible to detect the minimum detectable concentration of the examined gas with probability P , which is higher than the threshold probability P_0 . The threshold detection reliability P_0 was taken to be equal to 0.95.

5. SOLUTION OF THE INVERSE PROBLEM

The above-described analysis revealed the pronounced effect of the interfering gases CO_2 , H_2O , and CH_4 due to overlap of their absorption bands with the bands of the examined gases CO, NO, and NO_2 . Therefore for a quantitative analysis of CO, NO, and NO_2 the interfering gases must be also measured using the following channels: $\text{H}_2\text{O} - 1710 \text{ cm}^{-1}$, $\text{CH}_4 - 2990 \text{ cm}^{-1}$, and $\text{CO}_2 - 2430 \text{ cm}^{-1}$. Table II presents the absorption coefficients of all six gases at six wavelengths.

If we neglect the short-wave wing of the instrumental function in the CO measurement channel, then it is possible to derive a linear system of equations from Eq. (3) for determining the gas concentrations. The signals were calculated from formula (3) with the parameters $\eta = 50 \text{ mV}/(\text{mW}\cdot\text{cm}^{-1})$ and $W_0 = 1$ and 10 mW. The gas concentrations for which the absorption coefficients were calculated are listed in Tables III and IV in the first columns. For modeling the measurement noise the calculated OA signals were distorted using the generator of random variables with the parameters $(0, \sigma_a)$, where σ_a is the absolute error in measuring the OA signals ($\sigma_a = 2 \cdot 10^{-4} \text{ mV}$). The calculated results are given in Tables III and IV. The first columns of the tables give the exact values of gas concentrations in ppm., the second columns list the values obtained from the solution of the inverse problem averaged over 100 realizations, the third columns give the standard deviations, and the fourth columns show the relative errors. Given in the fifth columns are the numbers of the negative solutions while in the sixth columns are the data obtained with the error of more than 100%.

TABLE II. Matrix of the absorption coefficients ($\text{atm}^{-1}\cdot\text{cm}^{-1}$) with an account of the wing of the instrumental function.

ν, cm^{-1}	CO	NO	NO_2	H_2O	CO_2	CH_4
2110	1.69	$1.22 \cdot 10^{-6}$	0.0	$6.95 \cdot 10^{-4}$	$1.90 \cdot 10^{-3}$	$4.10 \cdot 10^{-7}$
1870	$2.75 \cdot 10^{-4}$	$9.46 \cdot 10^{-1}$	0.0	$6.97 \cdot 10^{-2}$	$1.22 \cdot 10^{-4}$	$3.49 \cdot 10^{-5}$
1600	0.0	$8.37 \cdot 10^{-5}$	$1.74 \cdot 10^1$	$4.39 \cdot 10^{-1}$	$6.98 \cdot 10^{-11}$	$2.30 \cdot 10^{-3}$
1710	$2.36 \cdot 10^{-9}$	$9.36 \cdot 10^{-3}$	$4.06 \cdot 10^{-3}$	$6.43 \cdot 10^{-1}$	$9.42 \cdot 10^{-8}$	$3.62 \cdot 10^{-4}$
2430	0.0	0.0	0.0	$1.06 \cdot 10^{-6}$	$2.31 \cdot 10^{-2}$	$1.82 \cdot 10^{-3}$
2990	0.0	0.0	$5.36 \cdot 10^{-4}$	$3.57 \cdot 10^{-3}$	0.0	1.39

TABLE III. The results of solving the inverse problem for the radiation power $W_0 = 1$ mW.

Gases	$\rho_{\text{acc}}, \text{ppm}$	$\rho_{\text{sol}}, \text{ppm}$	$\Delta_{\text{abs}}, \text{ppm}$	$\Delta_{\text{rel}}, \%$	N1	N2
CO	1.89	1.85	2.31	$5.95 \cdot 10^1$	21	42
NO	3.53	3.89	4.45	$4.12 \cdot 10^1$	21	45
NO_2	2.31	2.28	$2.98 \cdot 10^{-1}$	9.64	0	0
H_2O	$1.56 \cdot 10^2$	$1.57 \cdot 10^2$	6.49	3.88	0	0
CO_2	$1.00 \cdot 10^5$	$1.00 \cdot 10^5$	$1.80 \cdot 10^2$	$1.34 \cdot 10^{-1}$	0	0
CH_4	$1.00 \cdot 10^4$	$1.00 \cdot 10^4$	2.86	$1.94 \cdot 10^{-2}$	0	0

TABLE IV. The results of solving the inverse problem for the radiation power $W_0 = 10$ mW.

Gases	$\rho_{\text{acc}}, \text{ppm}$	$\rho_{\text{sol}}, \text{ppm}$	$\Delta_{\text{abs}}, \text{ppm}$	$\Delta_{\text{rel}}, \%$	N1	N2
CO	1.89	1.89	$2.31 \cdot 10^{-1}$	5.95	0	0
NO	3.53	3.57	$4.45 \cdot 10^{-1}$	4.12	0	0
NO_2	2.31	2.31	$2.98 \cdot 10^{-2}$	$9.64 \cdot 10^{-1}$	0	0
H_2O	$1.56 \cdot 10^2$	$1.56 \cdot 10^2$	$6.49 \cdot 10^{-1}$	$3.88 \cdot 10^{-1}$	0	0
CO_2	$1.00 \cdot 10^5$	$1.00 \cdot 10^5$	$1.80 \cdot 10^1$	$1.34 \cdot 10^{-2}$	0	0
CH_4	$1.00 \cdot 10^4$	$1.00 \cdot 10^4$	$2.86 \cdot 10^{-1}$	$1.94 \cdot 10^{-3}$	0	0

It can be seen from the tables that when the inverse problem is solved for CO and NO we obtain the largest error in reconstruction of the concentration. At the same time, negative values can appear for low concentrations of these gases ($2 \text{ mg}/\text{m}^3$ for CO and $4 \text{ mg}/\text{m}^3$ for NO) and $W_0 = 1$ mW. This is in a good agreement with the results of modeling the minimum detectable concentrations listed in Table I.

The accuracy of the solution can be increased by two methods. The first method is the use of regularizing algorithms for solving the inverse problem applying the *a priori* information about the sought-after concentrations (e.g., their positiveness). The second way is to increase the signal-to-noise ratio. Table IV lists the results of solving the inverse problem for $W_0 = 1$ mW which indicates a quite sufficient accuracy in determining the CO and NO concentrations.

REFERENCES

1. J. Christensen, in *Technical Review* (Bruel and Kjaer, Denmark, 1990), No. 1, pp. 1–39.
2. N.A. Borisevich, V.G. Vereshchagin, and M.A. Validov, *Infrared Filters* (Nauka i tekhnika, Minsk, 1971), 226 pp.

3. A.N. Zaidel', G.V. Ostrovskaya, and Yu.I. Ostrovskii, *Technology and Practice of Spectroscopy* (Nauka, Moscow, 1972), 332 pp.
4. M.M. Gurvich, *Photometry (Theory, Methods, and Instruments)* (Energoatomizdat, Leningrad, 1983), 272 pp.
5. L.S. Rothman, R.R. Gamache, and A. Goldman, *Appl. Opt.* **26**, No. 19, 4058–4097 (1987).
6. A.A. Mitsel' and K.M. Firsov, *Izv. Akad. Nauk SSSR, Fiz. Atmos. Okeana* **23**, No. 11, 1221–1227 (1987).
7. *Catalogue of Infrared Dispersive Filters in the Wavelength Range 4–30 μm* (Minsk, 1973).
8. M.Yu. Kataev and A.A. Mitsel', *Atm. Opt.* **4**, No. 7, 511–514 (1991).
9. B.R. Levin, *Theoretical Foundation of Statistical Radio-Engineering* (Sov. Radio, Moscow, 1985), Vol. 2.